Hydrosilation-Cured Poly(dimethylsiloxane) Networks: Intrinsic Contact Angles via Dynamic Contact Angle Analysis

Janelle M. Uilk,[†] Ann E. Mera,[‡] Robert B. Fox,[‡] and Kenneth J. Wynne*[,†]

Department of Chemical Engineering, School of Engineering, Virginia Commonwealth University, Richmond, Virginia 23284-3028, and Materials Chemistry Branch, Code 6120, Naval Research Laboratory, Washington, D.C. 20375

Received July 19, 2002

ABSTRACT: A method for measuring intrinsic advancing (θ_{adv}) and receding (θ_{rec}) water contact angles is reported for hydrosilylation-cured poly(dimethylsiloxane) network coatings that are analogues of biomedical materials. Static and dynamic contact angle (DCA) methods were used to evaluate coatings prepared from commercial divinyl-terminated poly(dimethylsiloxane) (C-DVPDMS) and synthesized low polydispersity divinyl-terminated poly(dimethylsiloxane) (N-DVPDMS). DCA measurements showed that coatings prepared with both C-DVPDMS and N-DVPDMS contaminated the water surface during analysis. For ambient temperature cure, the rate of contamination was C-DVPDMS > N-DVPDMS. Methods for acquiring intrinsic contact angles on the PDMS coatings include using a large surface area reservoir or changing the water reservoir between DCA cycles. Intrinsic contact angles for hydrosilylation-cured PDMS coatings are as follows: θ_{adv}, 118°, θ_{rec} 83°; after contamination of the water surface the contact angles change to θ_{adv}, 108°, θ_{rec} 87°.

Introduction

For decades, contact angles have been used to assess the wetting behavior of poly(dimethylsiloxane) containing polymers. Zisman relied on advancing contact angles (θ_{adv}) of various interrogating liquids to generate critical surface tensions of polymers including polyorganosiloxanes.[1,2] The fundamental molecular weight and chain end effects that modify the surface tension behavior of poly(dimethylsiloxane) liquids were examined by Koberstein.[3] Owen has reported contact angle measurements for silicon surfaces with grafted PDMS nanofilms.[4] θ_{adv} and θ_{rec} were dependent on the molecular weight of the PDMS graft.

Medical grade PDMS-based networks have been used for decades as soft tissue and joint replacement.[5,6] Contact angles have been used extensively to characterize PDMS implants or implant analogues.[7−9] Water contact angles were used by Kennan et al.[10,11] to estimate the degradation of medical grade silicones under oxidizing conditions. Medical grade PDMS materials utilized in implants continue to be under scrutiny with regard to biocompatibility and biodurability.[10,12]

We initiated work a number of years ago to clarify the wetting behavior of PDMS materials.[13,14] Problems encountered obtaining reproducible wetting behavior using goniometry led to the utilization of dynamic contact angle (DCA) analysis, that is, the Wilhelmy plate method. The DCA technique has been noted as a superior method for assessing wetting behavior.[15]

The extensive use of contact angles on PDMS materials leads us to report insidious water contamination effects discovered in the course of analyzing the wetting behavior of PDMS coatings. We did not recognize this contamination process in early work.[16] Taking into account rapid water contamination has led to a protocol for determination of intrinsic θ_{adv} and θ_{rec} for hydrosilylation cured PDMS coatings. Our work highlights the importance of checking interrogating liquid surface tension after exposure to a polymer film for assurance that the interrogating liquid has not been contaminated during contact angle analysis. The importance of this simple procedure rests in the likelihood of host contamination in an implant application if the polymer coating contaminates water in a DCA experiment.

Experimental Section

Materials. Commercial divinyl-terminated PDMS (C-DVPDMS) macromonomers (DMA-V31, 1000 cs, MW 28 000 and DMS−V22, 200 cs, MW 9400) were used as received from Gelest (Tullytown, PA). Molecular weights (MW) reported herein are manufacturers values. Trifunctional cross-linker, methyltris(dimethylsiloxy)silane ($MeSi(OSiMe_2H)_3$, XH_3), tetrafunctional cross-linker, tetrakis(dimethylsiloxy)silane ($Si(OSiMe_2H)_4$, XH_4), and platinum catalyst divinyltetramethyldisiloxane complex, 2−3% in xylene were also from Gelest. Platinum catalyst was further diluted with xylene to provide appropriate concentrations (typically 20 ppm Pt).

Synthesis of Narrow Polydispersity Divinyl-Terminated PDMS (N-DVPDMS). (1) Hexamethylcyclotrisiloxane (Aldrich, 98%) was purified prior to use by sublimation. DMSO was used as received from Aldrich, anhydrous, 99.8%. Toluene (Aldrich) was purified and dried prior to use by distilling from Na under nitrogen.

(2) Benzyltrimethylammonium bis(*o*-phenylenedioxy)-phenylsiliconate was synthesized according to the method of Lee[16] from catechol (60 mmol, Aldrich, 99+%), phenyltrimethoxysilane (30 mmol, United Chemical Technologies), and benzyltrimethylammonium hydroxide (30 mmol, Aldrich, 40 wt % solution in methanol) in methanol (30 mL). As per Lee,[16] white needle crystals were obtained that were recrystallized twice from methanol.

(3) Disilanol-terminated PDMS macromonomers were prepared from hexamethylcyclotrisiloxane using a modification of the method of Lee.[16] This method utilizes a benzyltrimethylammonium bis(*o*-phenylenedioxy)phenylsiliconate catalyst and dimethyl sulfoxide (DMSO) and water as cocatalysts. For each polymerization 5 g of hexamethylcyclotrisiloxane, 5 g of toluene, 2.26 mg of catalyst, 0.2 mL of DMSO, and 160 ppm of water were used with a reaction temperature of 60 °C. Reaction times for polymers with $M_n = 11\,700$ and $M_n = 24\,500$

[†] Virginia Commonwealth University.
[‡] Naval Research Laboratory.

10.1021/ma021154x CCC: $25.00
Published on Web 04/25/2003

were 20 and 35 min, respectively. Disilanol-terminated PDMS macromonomers were precipitated using methanol, separated, and dried in vacuo overnight.

(4) Disilanol-terminated PDMS macromonomers were converted to DVPDMS analogues by reaction with vinyldimethylchlorosilane in toluene using pyridine as an HCl acceptor.[17] A typical reaction utilized disilanol-terminated PDMS (4.5 g), 45 mL of toluene, 0.25 mL of vinyldimethylchlorosilane (5-fold excess), and 45 μL of pyridine (50% excess). The reaction was carried out at room temperature under nitrogen for 5 days. N-DVPDMS macromonomers were isolated by precipitation in methanol, separation, and vacuum-drying overnight.

GPC on a number of N-DVPDMS macromonomers gave polydispersities and M_n's that were the same as the parent diols, within experimental error. For preparation of N-PDMS coatings described herein, two N-DVPDMS macromonomers were used with molecular weights essentially identical to the N-PDMS diols described above.

Optimum Si—H to Vinyl Ratio. Broad MW distributions for C-DVPDMS macromonomers required an empirical determination of the optimum Si−H to vinyl ratio for network formation. This ratio was determined by estimating the Si−H to vinyl ratio that corresponded to elastomers with minimum extractable sol component and free Si−H.[15] Bulk hydrosilylation-cured samples were prepared following the same procedure described below for coatings. Following at least 24 h cure at ambient temperature, samples were placed in hexane. After swelling was complete (a minimum of 24 h), hexane was evaporated and extracted material was determined gravimetrically. These samples were also studied by infrared spectroscopy to examine the Si−H absorbance at 2130 cm^{-1}. Excess Si−H absorbance and sol fraction were minimized at Si−H/vinyl ratios from 1.4/1−1.7/1 with the optimum ratio being 1.5/1. In addition to broad MW distributions that made C-DVPDMS macromonomer equivalent weight uncertain, side reactions may consume excess Si−H.[18−20] These factors account for excess of Si−H needed for C-PDMS network formation.[21]

Coatings. In a typical coating preparation, 4 g of C- or N-DVPDMS was combined via hand stirring with 45 μL of XH_3 (Si−H/vinyl ratio of 1.5/1) and 2−3 mL of reagent grade hexane to slow gelation. When homogeneous, 20 ppm of catalyst was added via micropipet. The mixture was stirred until the viscosity increased (typically 4−5 min). Coverslips (Corning, 24 × 40 × 1.2 mm) were dip coated, taking care to distribute the coating evenly on both sides. The samples were placed in an upright position for cure at ambient conditions for at least 24 h prior to analysis.

Goniometry. Static contact angles were measured using an AST 2500 Video Contact Angle System (VCA). The water used for these measurements was triply distilled. Contact angles reported were the average of 6−8 drops.

Dynamic Contact Angle (DCA) Analysis. DCA determinations were carried out with a Cahn model 312 analyzer (Cerritos, CA) with a surface tension quantification limit of 0.1 dyn/cm. The DCA method is based on the Wilhelmy plate method.[22,23] The probe liquids were 18 MΩ/cm deionized water or saline-sodium citrate buffer 20× concentrate solution (Sigma) diluted with 18 MΩ/cm deionized water. Probe liquid surface tensions were checked daily. Typical values were 72.6 ± 0.1 dyn/cm for deionized water and 71.1 ± 0.1 dyn/cm for buffered saline solution.

Glassware used for DCA analysis was soaked in a 2-propanol/potassium hydroxide base bath for at least 2 h, rinsed for 30 s with hot tap water, rinsed another 30 s with Nanopure water, and flamed prior to use. When clean Nanopure water was used for a particular DCA, the beaker was also changed.

In a typical determination, a coated slide is attached to the electrobalance via a clip and the stage with the beaker of water is automatically raised and lowered to allow water to impinge upon the slide. By analyzing the resulting force vs distance curves (fdc's), θ_{adv} and θ_{rec} are obtained. Stage speeds were 100 μm/s unless otherwise noted. Dwell times between advancing and receding fdc's were either 60 or 10 s as indicated in figure captions or in the results and discussion.

Table 1. Contact Angles by Goniometry for C-PDMS Coatings for (A) MW 9400 C-DVPDMS/XH_4, (B) MW 28 000 C-dvpdms/Xh_3, and (C) MW 28 000 C-DVPDMS/XH_4

contact time of drop with surface (s)	static contact angle (deg)		
	A	B	C
0	115	122	114
30	109	120	107
60	107	114	106

Results

Divinyl-terminated PDMS (DVPDMS) was obtained commercially (C-DVPDMS) or was prepared by the method of Lee[16] (N-DVPDMS) to provide low polydispersity (1.1 vs PS calibration) macromonomers. Hydrosilylation-cured coatings were prepared using a molecular cross-linker $Me_nSi(OSiMe_2H)_{4-n}$ ($n = 0$, "XH_4" or 1, "XH_3")/and DVPDMS with Si−H to vinyl ratios at or near 1.5/1. This optimum ratio was established empirically by determining the Si−H to vinyl ratio that produced a PDMS network with negligible Si−H IR absorption and minimum hexanes−extractable sol.[15]

Goniometry. Contact angle data from goniometry is collected in Table 1 for C-PDMS coatings. The initial ($t = 0$) contact angle is ∼8° higher than the contact angle after 1 min. Loss of drop volume (∼1−2%) is minimal over this time. The decrease in initial contact angle prompted a closer investigation via dynamic contact angle (DCA) analysis to understand the change in contact angle with time. DCA utilizes coated slides with a much larger surface contact area between the wetting medium (water) and the sample. Evaporation of interrogating fluid is not a variable in DCA analysis.

DCA. A typical DCA result for a flamed glass slide and Nanopure water (surface tension 72.6 dyn/cm) is shown in Figure 1A. The superposition of fdc's for several cycles is characteristic of uncontaminated water. Representative DCA data for a C-PDMS coating is shown in Figure 1B. The first advancing force vs distance curve (fdc-a1) gives an advancing contact angle (θ_{adv}) of 116°. The three subsequent advancing fdc's give $\theta_{adv} = 107°$ while all of the receding fdc's yield $\theta_{rec} = 88°$. The 9° decrease in θ_{adv} from DCA is similar to the drop over 60 s in VCA goniometry.

After the DCA run shown in Figure 1B, the water surface tension was reexamined with a flamed glass slide (Figure 1C). In contrast to Figure 1A, the fdc's for three cycles (fdc-a + fdc-r = 1 cycle) give nonreproducible results with increasing contact angle hysteresis. The surface tension decreased with successive cycles (θ_{adv} = 72.6, 61.3, and 53.8 dyn/cm).

A new C-PDMS sample was run with the same water used for the DCA analysis shown in Figure 1B. The result is shown in Figure 1D ($\theta_{adv,1} = 113°$). A second DCA run for this sample in fresh Nanopure water gave fdc's nearly identical to those shown in Figure 1B. These experiments led to systematic changes in DCA protocols for elucidating the nature of suspected contamination effects.

Changing Water between Cycles. For the DCA data shown in Figure 2A, the water was changed prior to cycles 1, 2, and 5. Comparing the DCA data in Figure 2A with that of Figure 1B, two differences are observed. First, each time fresh water is introduced (prior to cycles 1, 2, and 5, Figure 2A), identical fdc's are observed. Second, in each of these cycles where water is changed before immersion, a new kind of behavior is observed in receding fdc's.

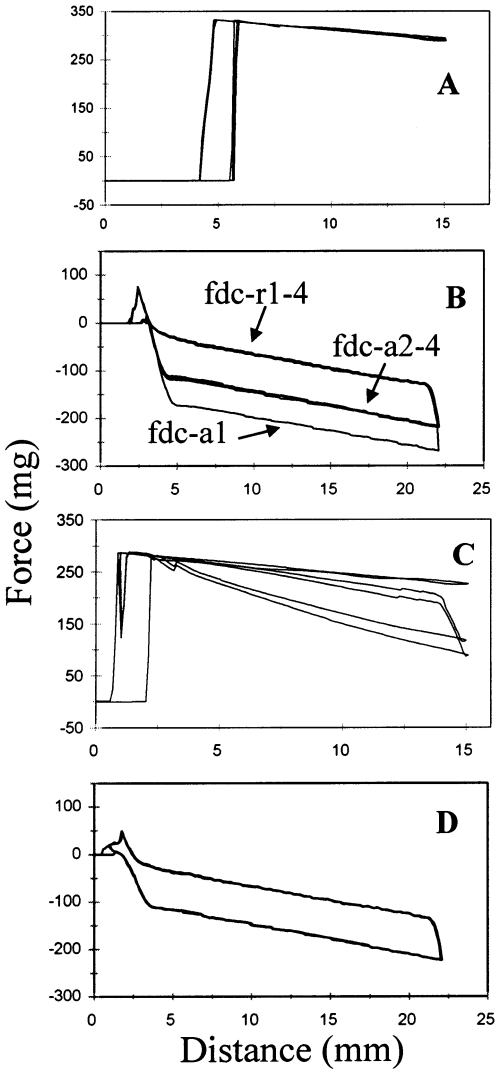

Figure 1. DCA: (A) flamed glass slide in clean beaker and water, (B) C-PDMS in beaker and water used for A, (C) flamed glass slide in beaker and water used for B, and (D) C-PDMS sample run in beaker and water used for A−C. In- and out-of-water dwell times were 10 s for A and C and 1 min for B and D.

Examining the wetting behavior in detail, fdc-a1 (Figure 2A) is identical to fdc-a1 in Figure 1B ($\theta_{adv,1}$ = 120°), but the first third of fdc-r1 is different, reflecting (temporarily) a higher force (lower θ_{rec}) before collapse. The extent of linearity is insufficient for calculation of an accurate θ_{rec}. Determination of an intrinsic θ_{rec} is discussed further below. Overall reproducibility is considered first.

The water change for the second cycle resulted in fdc-a2 being identical to fdc-a1. This result is in contrast to Figure 1B, wherein fdc-a1 was unique but where the water was not changed prior to fdc-a2. The third and fourth cycles shown in Figure 2A (fdc-a3 and fdc-r3; fdc-a4 and fdc-r4) were carried out without a water change. The fdc's for the third and fourth cycles yield contact angles (θ_{adv} = 108°, θ_{rec} = 89°) the same as those for the second through fourth cycles in Figure 1B. Importantly, when the water was changed for cycle 5 (Figure 2A), fdc-a5 and fdc-r5 returned to those observed for the first two cycles (Figure 2A, fdc-a1,2 and fdc-r1,2).

The reemergence of wetting behavior for cycle 5 identical to cycles 1 and 2 can only be explained by water contamination from the PDMS coating. The rate

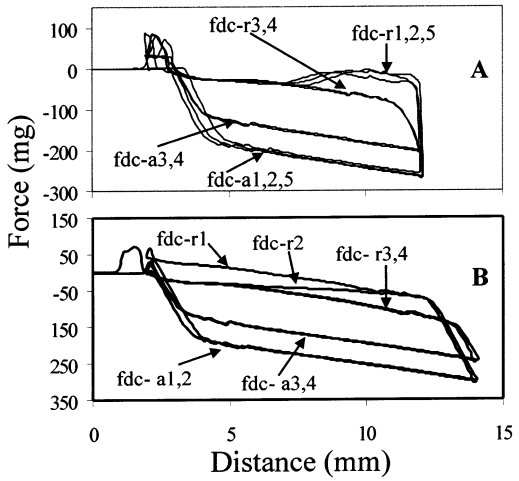

Figure 2. (A) DCA for C-PDMS. Fresh water and beaker introduced before fdc-a1,2,5 (in-air time was 20 s). In-water dwell time between fdc-a and fdc-r: 10 s. Vessel surface area: 12 cm^2. (B) DCA of C-PDMS with vessel surface area 74 cm^2. In- and out-of-water dwell times between were 10 s; 74 cm^2 surface area vessel was used.

of the contamination process is such that intrinsic advancing contact angles are observed each time the water is changed before a cycle. C-PDMS samples contaminate the water surface within 1−1$^1/_2$ min. Small quantities of water-soluble contaminants would have little effect on water surface tension. The reduction in surface tension is likely due to diffusion of siloxane species out of the coating. These species are insoluble in water and of lower density than water, causing them to migrate to the water surface.

The DCA data shown in Figure 2A employed a change in the in-water dwell time between sample immersion (fdc-a) and withdrawal (fdc-r) from 60 s (Figure 1) to 10 s. Compared to Figure 1B, the shorter in-water dwell allowed less time for water surface contamination before the receding force−distance determination. Thus, in Figure 2B the emergence of an intrinsic θ_{rec} on sample withdrawal is observed. An irreversible change occurs for fdc-r1, -2, and -5 before adequate linearity can provide an accurate θ_{rec}. A protocol is described in the next section for obtaining the intrinsic value of θ_{rec}.

Time Dependence of Water Contamination. If irreversible fdc change is due to formation of a PDMS-containing film on the water surface, and if the water-exposed coating surface area is constant, the time to collapse of initial fdc's should be dependent on water surface area. DCA analysis was therefore carried out utilizing a water reservoir with a larger surface area. A crystallizing dish with a surface area (sa) of 74 cm^2 proved convenient, compared to the beaker surface area (12 cm^2). Without any change of water, the 74 cm^2 sa container gave *two* identical advancing fdc's (θ_{adv} = 120°) and one receding fdc (θ_{rec} = 82°) prior to an irreversible change during fdc-r2 (Figure 2B). The contact angles for the subsequent cycles were $\theta_{adv3,4}$ = 110° and $\theta_{rec3,4}$ = 89°. These results provide evidence that employing the larger water surface area container delayed the onset of the fdc collapse.

DCA was carried out on a C-PDMS coating using a vessel of similar volume (300 mL) as the 74 cm^2 sa container but with a surface area of 20 cm^2. Collapse of the initial DCA curve occurred at 0.7 cycles (4 min) compared to 1.5 cycles (8 min) for the 74 cm^2 sa container (Table 2). Thus, fdc collapse depends on

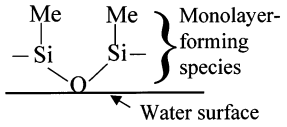

Figure 3. Depiction of the siloxane-containing monolayer (on water) used for thickness calculation.

Table 2. Time Required for Vessels of Differing Diameter to Contaminate the Water Surface, Where S Indicates Saline as the Interrogating Liquid

PDMS macromonomer	vessel surface area (cm^2)	time to contamination (min)	calculated mass 1 nm monolayer (μg)
commercial	12	3	1
narrow polydispersity	12	5	1
commercial	20	4	2
commercial (**S**)	74	9	8
commercial	74	9	8
commercial annealed (**S**)	74	10	8
commercial annealed	74	11	8
narrow polydispersity	74	16	8

surface area not container volume. Contact angles for cycle 1 in the 20 cm^2 sa vessel were $\theta_{adv} = 120°$ and $\theta_{rec} = 81°$. After collapse, contact angles for cycles 3−4 were $\theta_{adv3-4} = 111°$ and $\theta_{rec3-4} = 87°$. These post-collapse contact angles are virtually identical to those for C-PDMS using the 50 mL beaker (d = 3.9 cm, sa = 12 cm^2) and 74 cm^2 sa container.

Since the onset of collapse is taken as evidence for formation of a coherent film on the water surface, the amount of siloxane-containing species released from samples was estimated. Figure 3 illustrates in two dimensions a siloxane-containing species on the water surface. Using covalent and van der Waals radii, a 1 nm thickness is calculated.[24] This approximates the minimum thickness required for a coherent monolayer. For the 12 cm^2 sa vessel, only 1 μg of siloxane-containing species is required to form a monolayer, while 8 μg is required for 74 cm^2. Given the typical coating thickness (0.2 mm) and area in contact with water (31 cm^2), 8 μg is ∼0.05% of the coating mass.

C-PDMS Cure at 100 °C. A number of C-PDMS coatings were prepared (MW = 9400, Si−H/V ratio 1.7/1), cured at ambient temperature until nontacky (∼1 h), and then further cured at 100°C for 1 h. DCA measurements (74 cm^2 vessel) were carried out on 100 °C cured/annealed coatings and on identical ones cured at ambient temperature. DCA data for coatings cured at ambient temperature was identical to those previously presented (Figure 2B). DCA data of C-PDMS coatings cured/annealed at 100 °C (Figure 4A) show 2.5 cycles (11 min) before water contamination compared to 1.5 cycles (8 min) for nonheated analogues. Before contamination, $\theta_{adv1,2} = 116°$ and $\theta_{rec1,2} = 97°$ while after contamination $\theta_{adv3,4} = 108°$ and $\theta_{rec4} = 104°$.

The C-PDMS coatings cured/annealed at 100 °C took almost one full cycle longer to contaminate the water surface than those cured at ambient temperature. This is the longest time for any of the C-PDMS coatings. Curing/annealing at 100 °C apparently removes some contaminants or further cures the film, but does not prevent contamination. DCA analytical results were the same for measurements made 24 h and 2 wks after sample preparation.

Narrow-Polydispersity PDMS Samples. It is well-known that commercially available PDMS samples contain a significant fraction of low molar mass and linear siloxane species.[25,26] Therefore, divinyl-terminated PDMS, was synthesized by the method Lee[16] to provide low polydispersity PDMS macromonomers (N-DVPDMS). The synthetic method and the purification scheme for the N-DVPDMS macromonomers lead to very sharp GPC peaks and attendant low polydispersities (1.1 vs PS calibration). This approach was intended to minimize low molar mass constituents such as nonfunctional cyclics.

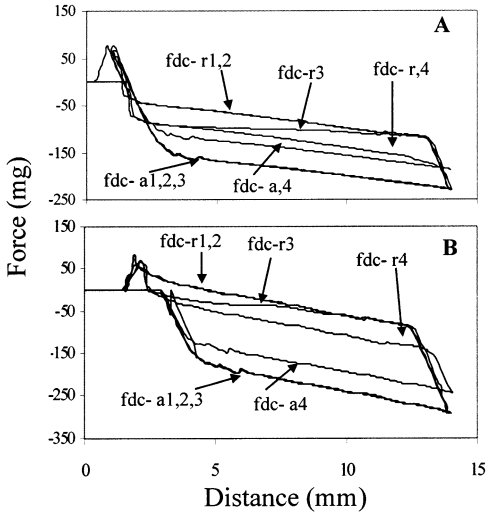

Figure 4. DCA using a 74 cm^2 surface area vessel for (A) C-PDMS, MW = 9400, Si−H/V = 1.7/1, 100 °C cure, and (B) N-PDMS, Mn = 11,700, Si−H/V = 1.5/1. In-water dwell time between fdc-a and fdc-r was 10 s.

Table 3. Contact Angles by Goniometry for (A) MW = 28 000 C-DVPDMS/XH_3, (B) M_n = 24 500 N-DVPDMS/XH_3, (C) MW = 9400, C-DVPDMS/XH_3, and (D) M_n = 11 700, N-DVPDMS/XH_3

contact time of drop with surface (s)	static contact angle (deg)			
	A	B	C	D
0	118	116	116	108
30	111	114	108	107
60	108	113	107	106

Coatings using C-DVPDMS and N-DVPDMS were prepared using the same cross-linker (XH_3), catalyst concentration (20 ppm), Si−H/vinyl ratio (1.5/1), and cure conditions (ambient temperature cure). Table 3 contains goniometry data for C-PDMS and N-PDMS coatings. The initial static contact angle for the N-PDMS coating is 108° and decreases 1−2° over 60 s. Initially, the C-PDMS coatings have contact angles of 116−118° and decrease to 107−113°.

The results of DCA analysis (Figure 4B) show that N-PDMS coatings provide 2.8 cycles (14 min) before irreversible water contamination. This is 1.3 cycles (5 min) longer to contaminate the water surface than comparable C-PDMS coatings run in the same diameter vessel (Figure 2B). Contact angles from DCA analysis for N-PDMS coatings are: before contamination, $\theta_{adv1,2,3} = 118°$ and $\theta_{rec1,2} = 86°$ while after contamination $\theta_{adv4} = 109°$ and $\theta_{rec4} = 93°$. Contact angle results for the C-PDMS coatings identical to those in Figure 2B were again obtained. Comparing the results of goniometry and DCA reinforces the analysis of Lander that DCA is a more reliable method for obtaining contact angles.[15]

Commercial PDMS Samples in Saline. Saline was used for DCA analysis to obtain results relevant to biomedical applications. Saline surface tension was 71.0 dyn/cm. For C-PDMS coatings prepared at ambient

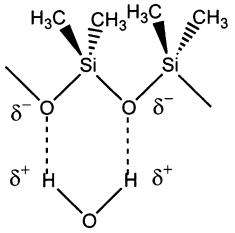

Figure 5. Depiction of electrostatic interaction of the Si−O−Si backbone with water.

temperature, contact angles prior to contamination were $\theta_{adv1,2} = 120°$ and $\theta_{rec1,2} = 88°$. After collapse, contact angles were $\theta_{adv4,5} = 109°$ and $\theta_{rec4,5} = 94°$. While θ_{adv} is within experimental error for PDMS coatings in water, θ_{rec} is about 5° higher than those in water. The result suggests that the PDMS surface is less wetted in saline than in water.

Additional experiments with saline included water changes before advancing cycles and surface tension measurements after DCA analysis. Results with saline were identical within experimental error to those obtained with water as the interrogating liquid. The time to contaminate saline by a C-PDMS sample is essentially the same as the time to contaminate water (Table 2).

Discussion

Intrinsic Wetting Behavior. Unfilled C-PDMS coatings cured at ambient temperature via hydrosilylation with molecular Si−H containing cross-linkers have intrinsic water contact angles of $\theta_{adv} = 118 \pm 2°$ and $\theta_{rec} = 83 \pm 2°$ based on 13 determinations. The contact angle hysteresis, $\Delta\theta$, is $35 \pm 4°$. Considering the chemical stability provided by hydrosilylation cure, the compositional simplicity, and the absence of filler and polar cross-linking moieties these values provide a convenient reference for comparing wetting behavior of other PDMS systems.

Contact angle hysteresis originates from minimization of interfacial tension in the interrogating fluid compared to air. As noted previously by Owen,[28] the presence of methyl groups at the air−polymer interface accounts for the high θ_{adv}. Once the PDMS surface is wetted, the polar Si−O−Si function is drawn to the water−polymer interface. The dipolar interactions of Si−O−Si and water are represented by structures such as that shown in Figure 5. Dipolar contributions account for the lower values of θ_{rec} as dipole−dipole interactions are lost when water dewets the surface. The observed contact angle hysteresis is independent of DCA stage speed from 60 to 160 μm/s. Lack of dependence of $\Delta\theta$ on stage speed reflects the low T_g (−120 °C) of the PDMS backbone.

Contamination Effects. Except for previous work on the surface science of condensation cured coatings using α,ω-dihydroxypoly(dimethylsiloxane),[14,29] the time-dependent effects of contamination on wetting behavior have not been investigated. However, oil release from PDMS elastomeric materials is well-known.[26,30−33] Varying protocols used for captive bubble, static or video contact angle, and dynamic contact angle determinations have apparently masked the effect of contamination on reported contact angles.

Our results may allow clarification of some of reports. For example, Kennan et al., reported the wetting behavior of Silastic (Silastic is a Dow Corning trademark) sheeting using both the underwater captive bubble and the sessile drop methods.[10] This material is a Pt-cured PDMS elastomer, but unlike the coatings reported herein, the Kennan Silastic is filled with fumed silica (25%). The captive bubble method resulted in θ_{adv} of 121−123°, while the sessile drop method resulted in $\theta_{adv} = 112-115°$.[10] These systematic differences in θ_{adv} may be due to water contamination effects. During the captive bubble technique, the siloxane-containing species would have to travel against gravity to reach the interface between the air bubble and water. This geometric arrangement works against contamination of the water−air interface and may account for the observation of intrinsic θ_{adv}. An opposite arrangement exists for the sessile drop method, where the lower density siloxane-containing species travel quickly to the surface of the water drop. The systematically lower θ_{adv} reported using the sessile drop method may thus reflect contamination effects.

Table 4. Comparison of Previously Reported Contact Angles (deg) on PDMS Elastomers

type of PDMS sample	contact angle measurement method	contact angle θ_{adv}	contact angle θ_{rec}	ref
hydrosilation cured	sessile drop	103	93	Olander[36]
hydrosilation cured	sessile drop	118	90	Perutz[34]
hydrosilation cured	sessile drop	100−105	75−80	Hillborg[30]

Perutz et al. (Table 4) used the sessile drop technique on hydrosilylation cured PDMS films that had been extracted in toluene ($\theta_{adv} = 118°$ and $\theta_{rec} = 90°$).[34,35] The θ_{adv} is the same as our DCA result, indicating that extraction of cured PDMS samples can allow measurement of intrinsic contact angles. However, extraction does not ensure measurement of intrinsic wetting behavior. Other sessile drop measurements (Table 4) on hydrosilylation cured PDMS samples purified by Soxhlet extraction show a range in values for θ_{adv} and θ_{rec}.[30,36] Our attempts to carry out DCA analysis on C-PDMS coatings extracted with hexane failed as the coatings suffered adhesive failure at the glass-coating interface during swelling. After removal of solvent, the coatings were distorted.

Conclusions

A protocol for evaluating wetting behavior of hydrosilylation cured PDMS coatings was developed that allows the determination of whether surface contamination of water occurs. Contamination of the water surface is characterized by an irreversible change in θ_{adv} and θ_{rec} over a series of DCA cycles. Contamination is clearly evidenced by deviations from coincident advancing and receding fdc's. Surface water contamination is readily detected by measuring water surface tension of the post-DCA test water with a flame-dried glass slide. Surface contamination is indicated by a dependence of wetting behavior on the surface area of the water reservoir. If a pristine coating is evaluated with water previously used, intrinsic wetting behavior is not observed. Water contamination was found not only for coatings prepared with commercial DVPDMS macromonomer but with specially synthesized, narrow polydispersity (1.1) DVPDMS, though the contamination rate was slower for the latter coatings.

Changes in wetting behavior due to water contamination stand in contrast to changes in wetting behavior that occur due to slow surface structure reorganization. Surface reorganization in water is characterized by

decreasing θ_{adv} and θ_{rec} with immersion time. Such changes are observed for polyurethanes, acrylates and other polymers that can hydrogen bond with water.[37−39] Favorable enthalpy drives reorganization, with the rate depending on surface mobility. However, if the coating does not contaminate water and if surface mobility is sufficient, intrinsic θ_{adv} and θ_{rec} are restored, usually by drying in air. Until contamination effects occur, C-PDMS coatings display stable intrinsic values for θ_{adv} and θ_{rec}. Contact angle hysteresis ($35 \pm 4°$) is therefore also stable because PDMS has a very low T_g making the time scale of surface reorganization many orders of magnitude faster than the switch from advancing to receding force−distance determinations.

The water/saline contamination effect observed for PDMS coatings has implications for biomaterials evaluation. The importance of the protocol for detecting contamination rests in the likelihood that if a polymer coating contaminates water or saline in a DCA experiment, it is likely to contaminate a host in an implant application. Our results with PDMS-based coatings have prompted us to examine the wetting behavior of other biomedical polymers for intrinsic and extrinsic effects on wetting behavior. Present work focuses on polyurethanes and will be reported in due course.

Acknowledgment. The authors thank the Office of Naval Research, the Strategic Environmental Research and Development Program (SERDP), the VCU School of Engineering Foundation, and the National Science Foundation for support of this research.

References and Notes

(1) Fox, H. W.; Taylor, P. W.; Zisman, H. W. *Ind. Eng. Chem. Res.* **1947**, *39*, 1401.
(2) Zisman, H. W. *Advances in Chemistry*; American Chemical Society: Washington, DC, 1964; Vol. 43.
(3) Jalbert, C.; Koberstein, J. T.; Yilgor, I.; Gallagher, P.; Krukonis, V. *Macromolecules* **1993**, *26*, 3069−3074.
(4) She, H.; Chaudhury, M. K.; Owen, M. J. *Polym. Prepr.* **1998**, *39*, 548.
(5) Swanson, A. B. *Int. Clin. Inf. Bull.* **1966**, *6*, 16−19.
(6) Arkles, B. *CHEMTECH* **1983**, *13*, 542−555.
(7) Everaert, E.; Van de Belt-Gritter, B.; Van der Mei, H. C.; Busscher, H. J.; Verkerke, G. J.; Dijk, F.; Mahieu, H. F.; Reitsma, A. *J. Mater. Sci.—Mater. Med.* **1998**, *9*, 147−157.
(8) Waters, M.; Jagger, R. *J. Biomed. Mater. Res.* **1999**, *48*, 765−771.
(9) Waters, M. G. J.; Jagger, R. G.; Polyzois, G. L. *J. Prosthet. Dent.* **1999**, *81*, 439−443.
(10) Kennan, J. J.; Peters, Y. A.; Swarthout, D. E.; Owen, M. J.; Namkanisorn, A.; Chaudhury, M. K. *J. Biomed. Mater. Res.* **1997**, *36*, 487−497.
(11) Batich, C.; DePalma, D.; Marotta, J.; LaTorre, G.; Hardt, N. S. *Curr. Top. Microbiol. Immunol.* **1996**, *210*, 13−23.
(12) Wolf, C. J.; Jerina, K. L.; Brandon, H. J.; Young, V. L. *J. Biomater. Sci.—Polym. Ed.* **2001**, *12*, 801−815.
(13) Pike, J. K.; Ho, T.; Wynne, K. J. *Chem. Mater.* **1996**, *8*, 856−860.
(14) Johnston, E.; Bullock, S.; Uilk, J.; Gatenholm, P.; Wynne, K. J. *Macromolecules* **1999**, *32*, 8173−8182.
(15) Mera, A. E.; Fox, R. B.; Bullock, S.; Wynne, K. J. In *Proceedings of the American Chemical Society Division of Polymeric Materials: Science and Engineering*; American Chemical Society: Washington, DC, 1997; Vol. 77, pp 636−637.
(16) Lee, C. L.; Johannson, O. K. *J. Polym. Sci., Polym. Chem.* **1976**, *14*, 729.
(17) Patel, S. K.; Cohen, C. *Macromolecules* **1992**, *25*, 5252.
(18) Lestel, L.; Cheradame, H.; Boileau, S. *Polymer* **1990**, *31*, 1154.
(19) Britcher, L. G.; Kehoe, D. C.; Matisons, J. G.; Swincer, A. G. *Macromolecules* **1995**, *28*, 3110.
(20) Marko, I. E.; Sterin, S.; Buisine, O.; Mignani, R.; Branlard, P.; Tinant, B.; Declercq, J. P. *Science* **2002**, *298*, 204−206.
(21) Olander, B. W.; A.; Albertsson, A.-C. *Biomacromolecules* **2003**, *4*, 145−148.
(22) Johnson, R. E., Jr.; Dettre, R. H. In *Surfactant Science Series*; Berg, J. C., Ed.; M. Dekker: New York, 1993; Vol. 49, pp 1−73.
(23) Adamson, A. W.; Gast, A. P. *Physical Chemistry of Surfaces*; 6th ed.; John Wiley and Sons: New York, 1997.
(24) Demitras, G. C.; Russ, C. R.; Salmon, J. F.; Weber, J. H.; Weiss, G. S. *Inorganic Chemistry*; Prentice-Hall: Englewood Cliffs, NJ, 1972.
(25) Carmichael, J. B.; Winger, R. *J. Polym. Sci., Polym. Chem.* **1965**, *3*, 971−981.
(26) Compton, R. A. *J. Long-Term Eff. Med. Implants* **1997**, *7*, 29−54.
(27) Lander, L. M.; Siewerski, L. M.; Brittain, W. J.; Vogler, E. A. *Langmuir* **1993**, *9*, 2237.
(28) Owen, M. J. In *Silicon-Based Polymer Science A Comprehensive Resource*; Zeigler, J. M.; Fearon, F. W., Eds.; American Chemical Society: Washington, DC, 1990; Vol. 224.
(29) Uilk, J.; Bullock, S.; Johnston, E.; Myers, S. A.; Merwin, L. H.; Wynne, K. J. *Macromolecules* **2000**, *33*, 8791−8801.
(30) Hillborg, H.; Sandelin, M.; Gedde, U. W. *Polymer* **2001**, *42*, 7349−7362.
(31) Hillborg, H.; Gedde, U. W. *Polymer* **1998**, *39*, 1991−1998.
(32) Kim, J.; Chaudhury, M. K.; Owen, M. J.; Orbeck, T. *J. Colloid Interface Sci.* **2001**, *244*, 200−207.
(33) Kim, J.; Chaudhury, M. K.; Owen, M. J. *J. Colloid Interface Sci.* **2000**, *226*, 231−236.
(34) Perutz, S.; Kramer, E. J.; Baney, J.; Hui, C. Y. *Macromolecules* **1997**, *30*, 7964−7969.
(35) Perutz, S.; Kramer, E. J.; Baney, J.; Hui, C. Y.; Cohen, C. *J. Polym. Sci., Part B: Polym. Phys.* **1998**, *36*, 2129−2139.
(36) Olander, B.; Wirsen, A.; Albertsson, A. C. *Biomacromolecules* **2002**, *3*, 505−510.
(37) Tingey, K. G. A.; J. D. *Langmuir* **1991**, *7*, 2471−2478.
(38) Tretinnikov, O. N.; Ikada, Y. *Langmuir* **1994**, *10*, 1606−1614.
(39) Makal, U.; Wynne, K. J. Unpublished results.

MA021154X